Domain Sensitive Contrast in Photoelectron Emission Microscopy

D. Thien,* P. Kury, M. Horn-von Hoegen, and F.-J. Meyer zu Heringdorf
Fachbereich Physik und CeNiDE, Universität Duisburg-Essen, Campus Duisburg, 47057 Duisburg, Germany

J. van Heys, M. Lindenblatt, and E. Pehlke
Institut für Theoretische Physik und Astrophysik, Universität Kiel, 24098 Kiel, Germany
(Received 19 January 2007; published 7 November 2007)

We have investigated the adsorption of cesium on the Si(100) surface with photoelectron emission microscopy using linearly polarized green laser light. We observe a polarization dependent contrast between the (2×1) or (1×2) reconstructed terraces. Density-functional calculations reveal the geometric and electronic structure of the Cs/Si(100) surface. The contrast between the (2×1) or (1×2) reconstructed domains is explained on the basis of dipole selection rules for the photoemission matrix elements.

DOI: 10.1103/PhysRevLett.99.196102 PACS numbers: 68.37.Xy, 68.43.Bc, 73.20.At, 79.60.Dp

Surface spectromicroscopy, i.e., the combination of surface-sensitive spectroscopic techniques with spatial resolution, has become very fashionable during the last several years. Using synchrotron light sources, for instance, chemical [1] or magnetic [2] contrast can be obtained with photoelectron emission microscopes (PEEMs). The combination of lasers with the PEEM will allow the study of polarization effects in valence-band spectromicroscopy with high spatial and energetic resolution with laboratory sources. For instance, a focused green laser pointer offers already a flux of linearly polarized photons that is several orders of magnitude higher than what can be achieved in the state-of-the-art beam lines. Such light offers novel contrast mechanisms in PEEM. In this Letter we describe a yet unrecognized contrast mechanism due to matrix element dependence of orthogonal surface domains on the polarization of the incident light. The system studied is the cesiated (2×1) reconstructed Si(001) surface. The work function of the Si(001) sample has been lowered by adsorption of 0.5 ML Cs in such a way that photoemission becomes energetically possible even for green laser light. The surprising finding of domain contrast (see Fig. 1) on the cesiated Si(001) surface is explained on the basis of the band structure as obtained from density-functional theory (DFT), together with dipole selection-rules from photoemission theory.

The experiments were carried out in ultrahigh vacuum (UHV, base pressure below 1×10^{-10} mbar) using an ELMITEC PEEM III with imaging energy analyzer [3]. For illumination of the sample a Coherent Verdi V8 Nd: YVO_4 laser (532 nm, cw) with an angle of incidence of 74° relative to the surface normal was used. The substrates were cut from a Boron-doped Si(100) wafer (8–12 Ω cm, Wafernet), wiped off with isopropanol, and degassed at 800 K for several hours after insertion into the UHV. The native oxide was removed by repeated flash-annealing yielding an atomically clean surface. Cs was deposited from well-outgassed chromate dispensers (SAES getters).

Figure 1 shows a PEEM micrograph in which the two either (1×2) or (2×1) reconstructed terraces of the Si(100) surface are clearly distinguishable from each other. Upon room temperature (RT) adsorption of Cs on Si(100) the photoelectric work function of the surface is lowered by 3.3 eV [4,5]. We identified the Cs saturation coverage

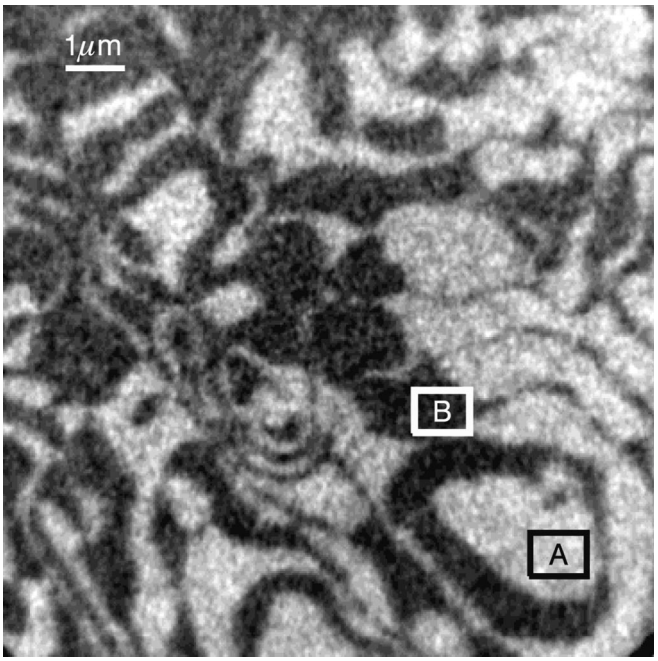

FIG. 1. PEEM image of the cesiated Si(100) surface at room temperature using linearly polarized green laser light. The two different types of terraces (A and B) show different photoemission yield depending on the polarization of the incident light. The shown figure is an asymmetry image between a micrograph taken with *p*-polarized light and one taken with *s*-polarized light to enhance the contrast.

according to literature [4] by measuring the work function change during Cs adsorption, which we deduce from the change in width of the photoelectron spectrum. At saturation coverage (0.5 ML at RT [6], equivalent to one Cs adatom per (2×1)-cell), the work function reaches a minimum. The (2×1) reconstruction of the Si(100) substrate stays intact throughout the experiment as has been confirmed by low energy electron diffraction (LEED). Moreover, the step morphology of the clean Si(100) surface remains unaltered by the adsorption of Cs on Si(100) as we confirmed by low energy electron microscopy (LEEM). Under dark-field conditions in LEEM one of the two domains is imaged bright, the other one dark. Just before reaching saturation coverage, a similar domain contrast can be observed in PEEM (Fig. 1). The contrast remains during further adsorption of up to approximately one monolayer of cesium. As can be deduced from the coverage dependant change in work function during cesium adsorption on Si(100) [4,5], a photoemission signal can only be expected from $\theta \approx 0.3$ ML on due to the limited energy of the incoming light (2.33 eV). During deposition additional Cs atoms adsorb onto the 0.5 ML Cs/Si(100) surface. These atoms desorb again when the Cs flux is turned off to return to saturation coverage. Between $\theta \approx 0.3$ ML and more than 0.5 ML the domain contrast changes only in intensity. This variation is attributed to the variation of the photoelectron yield, which is largely determined by the coverage-dependent work function.

The domain contrast in PEEM exhibits a strong dependence on the polarization direction of the incident laser light. Turning the polarization of the incoming laser light by 90° gradually changes the dark-bright contrast until it is finally inverted. Figure 2 shows the intensity difference between a dark and a bright area on the surface as a function of the polarization angle φ [7].

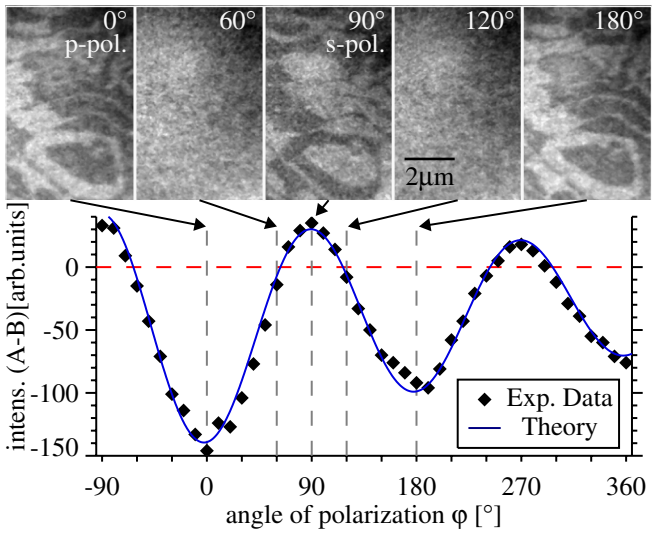

FIG. 2 (color online). Polarization dependence of domain contrast between areas A and B from Fig. 1. The solid line is a fit to the data according to Eq. (3) together with an additional exponential decay due to the slight desorption of Cs during the experiment.

The geometric and electronic structure of cesiated Si(001) surfaces has been calculated *ab initio* employing the DFT total-energy package FHI96MD [8]. We use norm-conserving Hamann pseudopotentials for Si and Cs. A Cs pseudopotential has been generated [9], in which the 6*s* together with the six 5*p* electrons are treated as valence electrons, and the nonlinear core-valence exchange-correlation correction is taken into account. Exchange and correlation are treated within the generalized gradient approximation [10].

Our DFT calculations refer to a Cs-coverage of 0.5 ML, corresponding to one Cs atom per Si surface dimer. Beyond recent DFT calculations assuming a (2×1) surface unit cell [11,12] we use a twice as large $p(2 \times 2)$ surface unit cell in order to allow for additional Jahn-Teller distortions. We use a plane-wave cutoff-energy of 30 Ry and at least 16 special **k** points [13] in the irreducible part of the Brillouin zone. The slab thickness amounts to 16 Si layers, with Cs atoms adsorbed on either side. Various adsorption configurations corresponding to Cs atoms located at the cave ($T4$), valley bridge ($T3$), pedestal, and bridge sites [14] have been fully relaxed. The valley-bridge structure yields the energetically most preferred Cs adsorption site. We find two inequivalent Si dimers in the $p(2 \times 2)$ cell, one with a buckling angle of 12°, displaying the characteristic local electronic structure of occupied and unoccupied rehybridized dangling-bond orbitals, and one nearly symmetric dimer with a buckling angle less than 2° with two filled dangling-bond orbitals, a π-bonding, and a π^*-antibonding one. Apparently this antibonding orbital on the nearly symmetric dimer has become occupied with electrons from the two Cs atoms in the (2×2) unit cell. The actual charge transfer, however, cannot easily be derived from the calculations, due to the diffuse nature of the Cs 6*s* state. Altogether, the additional relaxation in the (2×2) cell, as opposed to the smaller (2×1) cell, lowers the energy by 35 meV per Si dimer. As this energy gain is quite small, the surface at RT is likely to have undergone a transition into a phase, where the Si dimers move randomly and which is (1×2) on statistical average, which would reconcile our calculations with experimental observations.

Photoemission is discussed on the basis of the Kohn-Sham band structure calculated at $T = 0$ K. Unlike the necessarily metallic band structure of the (1×2)-reconstructed surface [11,12], the band structure in Fig. 3 is semiconducting. From inspection of the electronic states within the fundamental gap we find that the occupied surface states are predominantly derived from Si dangling-bond orbitals. Relevant Cs admixtures occur only for surface states above the Fermi level.

That part of the valence-band structure from which electrons excited by photons with an energy of 2.33 eV

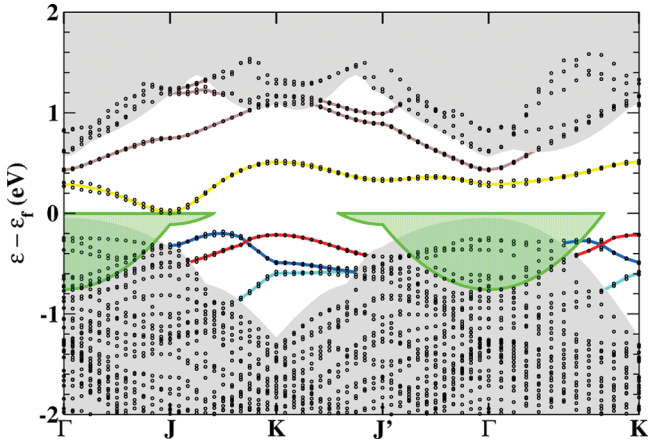

FIG. 3 (color). Kohn-Sham band-structure of the Cs/Si(001) surface at 0.5 ML coverage in valley-bridge adsorption geometry. Brown marked surface bands are characterized by Cs states, the yellow marked band is derived from the empty p-like state at the lower Si atom of the buckled dimer. The blue surface bands are derived from the filled states at the upper Si-dimer atom and the π bonding state at the symmetric dimer. The red marked surface band is characterized by a π^*-antibonding state at the symmetric dimer. The green hatched area denotes that part of the band-structure from which electrons excited with a 2.33 eV photon can be emitted into the vacuum.

can be emitted into the vacuum is hatched in green in Fig. 3. This region is further narrowed by the acceptance cone of the PEEM: Only 18% of the surface Brillouin zone of the $p(2 \times 2)$ cell around the Γ point can be imaged. Thus mainly electrons from a region around the Γ point are collected by the PEEM. From energy conservation, together with a theoretical work function of 1.6 eV, a photon energy of 2.33 eV, and in view of quasiparticle corrections of the eigenenergies missing in the Kohn-Sham picture, we conclude that for the $p(2 \times 2)$ reconstructed surface the π^* resonance at Γ appears to be slightly too low in energy (0.6–0.8 eV below the valence-band edge) to be imaged by the PEEM. However, within the full Brillouin zone the occupied π^*-band disperses close to the valence-band edge. Because of either the backfolding of the surface band structure in the large (8×4) reconstruction as reported by Abukawa *et al.* [15], or due to strong diffuse electron scattering by the not well-ordered Cs/Si surface structure as suggested by the intense diffuse background in the LEED images at room temperature, electrons derived from the occupied π^*-states will be scattered into the Γ point of the surface Brillouin zone. This is consistent with the observation of the PEEM contrast for a range of Cs coverage, which apparently is only limited by the variation of the surface work function. Over this range of coverages, various surface reconstructions have been reported [15,16]. Thus the contrast mechanism is not expected to sensitively depend on the size of any particular surface reconstruction. The conclusion from our Kohn-Sham band structure is thus the existence of occupied π^* states in the density of states close to the valence-band edge. We will now investigate the role of these states for the formation of PEEM contrast between differently oriented Cs/Si(001) surface domains.

Because of Si space-group symmetry, bulk contributions basically do not change when the crystal is rotated by 90° around the surface normal; thus, they are not expected to contribute to the observed PEEM domain contrast.

The photocurrent can be described by a golden rule formula [17], with v_e denoting the velocity of the photoelectron:

$$j \sim v_e \sum_i^{\text{occ}} |\langle f|\mathbf{A}\cdot\mathbf{p} + \mathbf{p}\cdot\mathbf{A}|i\rangle|^2 \delta(\varepsilon_f - \varepsilon_i - \hbar\omega). \quad (1)$$

We apply the dipole approximation to the photoemission matrix element, which is accurate for the long wavelengths considered here. In the case of normal emission, the final state $|f\rangle$ is trivially symmetric with respect to all two-dimensional symmetry transformations of the crystal filling the half space. The π and π^* initial states $|i\rangle$ are formed from Si dangling bonds and are symmetric (positive parity) with respect to mirror planes perpendicular to the Si surface that include the Si dimer. Consequently, the photoemission matrix elements vanish for components of the vector potential $\mathbf{A}$ perpendicular to this mirror plane. If, for simplicity, we furthermore consider an additional *approximate* mirror plane perpendicular to the symmetric Si dimer, we can assume that for the π^* state, which has negative parity with respect to this second mirror plane [18], the photoemission matrix element will be negligible for the component of $\mathbf{A}$ perpendicular to the crystal surface, while it will presumably be large for the component parallel to the dimer bond. On the other hand, the π state has a positive parity also with respect to this second mirror plane; hence, its photoemission matrix elements will vanish for any vector potential lying fully in the surface plane. We conclude that the π^* state is—in view of the dimer buckling not the only one but the most probable candidate—responsible for the observed polarization contrast. This is further corroborated by the fact that the PEEM contrast is observed even for Cs coverages close to 1 ML, for which all Si dimers are nearly symmetric [11].

Let us for simplicity assume that the difference in photoemission intensity between the (1×2) and (2×1) dimerized terraces is due to photoemission from states for which only the photoemission matrix element for $\mathbf{A}$ parallel to the dimer bonds of the symmetric dimers is nonvanishing. As explained above, this holds true for π^*-antibonding states localized at the Si dimer, if there are two orthogonal mirror planes perpendicular to the surface. In this case the polarization dependence of the PEEM contrast can be traced back to the variation of the respective field components of the light wave. We apply the Fresnel formulas with a dielectric constant $n(\omega) \approx 4.21$ [19] to roughly account for dielectric effects and

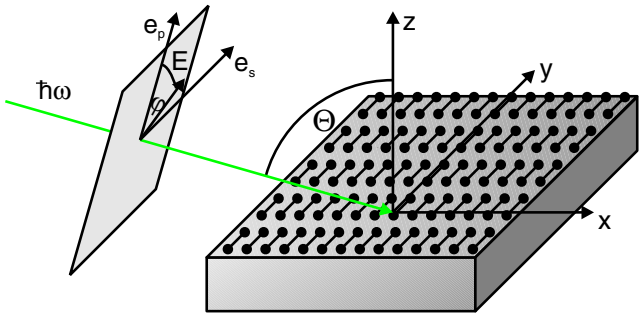

FIG. 4 (color online). Definition of the angle of polarization φ and angle of incidence of the light θ.

calculate the electric field just outside the Si crystal,

$$\mathbf{E}(x, y, z = 0^+) \sim \mathrm{Re}\{[(1 - r_p)\cos\varphi\cos\theta\hat{\mathbf{e}}_\mathbf{x} + (1 + r_s)\sin\varphi\hat{\mathbf{e}}_\mathbf{y} + (1 + r_p)\cos\varphi\sin\theta\hat{\mathbf{e}}_\mathbf{z}]e^{i(k_x x - \omega t)}\}, \quad (2)$$

with the reflectivities r_p and r_s for p- and s-polarized light. See Fig. 4 for the definition of the angles θ and φ. Inserting this expression for the electric field into Eq. (1) for the photocurrent and assuming two orthogonal mirror planes as discussed above, we find that the PEEM contrast, i.e., the difference Δj in photocurrent from different domains on the surface, is proportional to the difference of the squares of the electric field components parallel and perpendicular to the direction of dimerization in the surface,

$$\Delta j \sim -(|1 + r_s|^2 - |1 - r_p|^2\cos^2\theta) + (|1 + r_s|^2 + |1 - r_p|^2\cos^2\theta)\cos(2\varphi). \quad (3)$$

We have fitted the experimentally observed data for the PEEM contrast using Eq. (3). Note, that the only free parameter is the overall proportionality factor. However, due to slight Cs desorption the intensity drops during the measurement, which has been considered by an additional exponential decay. The resulting fit is displayed as the full line in Fig. 2 and shows excellent agreement with the experimental data.

In conclusion, the polarization dependence of the PEEM contrast originates from the photoemission matrix elements of the Si dangling-bond states. In case of normal photoelectron emission these can easily be analyzed via dipole selection rules. The role of the Cs adsorbate is, first of all, to form a surface dipole layer which drastically lowers the work function, thus making photoemission with light in the visible range feasible. Furthermore, the Cs atoms donate electrons into π^* antibonding Si-dimer states of the Si(001) surface, which are shown to contribute to the PEEM contrast. According to the dipole selection rules, the terrace with the dimer bond parallel to the incoming electric field vector has the higher photoelectron yield, as has been confirmed by the typical elliptical shape of Si islands [20]. The dark-bright-contrast can be inverted by changing the polarization angle of the linearly polarized light by 90°, in accordance with the symmetry of the occupied π^* surface state. Using synchrotron radiation of necessarily higher photon energy for illumination, a similar contrast ought to be observable, assuming that an energy analyzer is used to select the π^* antibonding Si-dimer states for imaging. However, with the flux of linearly polarized photons at a synchrotron being orders of magnitude smaller than that of even a laser pointer, the exposure times to obtain a comparable observation would become unreasonable.

We thank R. van Gastel and ELMITEC for assistance in determining the acceptance cone of the PEEM. Financial support by the Deutsche Forschungsgemeinschaft under Sonderforschungsbereich 616 "Energy Dissipation at Surfaces" is gratefully acknowledged.

*dagmar.thien@uni-due.de

[1] F.-J. Meyer zu Heringdorf *et al.*, Phys. Rev. Lett. **86**, 5088 (2001).
[2] F. Nolting *et al.*, Nature (London) **405**, 767 (2000).
[3] T. Schmidt *et al.*, Surf. Rev. Lett. **5**, 1287 (1998).
[4] J. E. Ortega *et al.*, Phys. Rev. B **36**, 6213 (1987).
[5] V. Zielasek *et al.*, Phys. Rev. B **72**, 115422 (2005).
[6] W. B. Sherman *et al.*, Phys. Rev. B **62**, 4545 (2000).
[7] See also the movie in EPAPS Document No. E-PRLTAO-99-031743 for more information on EPAPS, see http://www.aip.org/pubservs/epaps.html.
[8] M. Bockstedte *et al.*, Comput. Phys. Commun. **107**, 187 (1997).
[9] M. Fuchs and M. Scheffler, Comput. Phys. Commun. **119**, 67 (1999).
[10] J. P. Perdew, K. Burke, and M. Ernzerhof, Phys. Rev. Lett. **77**, 3865 (1996).
[11] R. Shaltaf, E. Mete, and S. Ellialtioğlu, Phys. Rev. B **72**, 205415 (2005).
[12] H. Y. Xiao *et al.*, J. Chem. Phys. **122**, 174704 (2005).
[13] H. J. Monkhorst and J. D. Pack, Phys. Rev. B **13**, 5188 (1976).
[14] See EPAPS Document No. E-PRLTAO-99-031743, Fig. 1 for geometry of surface unit cells of the different adsorption sites. For more information on EPAPS, see http://www.aip.org/pubservs/epaps.html.
[15] T. Abukawa, T. Okane, and S. Kono, Surf. Sci. **256**, 370 (1991).
[16] T. Abukawa and S. Kono, Surf. Sci. **214**, 141 (1989).
[17] *Solid-State Photoemission and Related Methods*, edited by W. Schattke and M. van Hove (Wiley-VCH, New York, 2003).
[18] See EPAPS Document No. E-PRLTAO-99-031743, Figs. 2 and 3 for electron densities of π and π^* states. For more information on EPAPS, see http://www.aip.org/pubservs/epaps.html.
[19] D. E. Aspnes and A. A. Studna, Phys. Rev. B **27**, 985 (1983).
[20] R. M. Tromp and M. C. Reuter, Phys. Rev. B **47**, 7598 (1993).